Study of pressure effect on the magnetic penetration depth in MgB_2

D. Di Castro,[1,2,*] R. Khasanov,[1,3] C. Grimaldi,[4] J. Karpinski,[5] S. M. Kazakov,[5] and H. Keller[1]

[1] *Physik-Institut der Universität Zürich, Winterthurerstrasse 190, CH-8057 Zürich, Switzerland*
[2] *INFM-Coherentia and Dipartimento di Fisica, Universita' di Roma "La Sapienza", P.le A. Moro 2, I-00185 Roma, Italy*
[3] *Paul Scherrer Institute, CH-5232 Villigen PSI, Switzerland*
[4] *Ecole Polytechnique Fédérale de Lausanne, LPM, CH-1015 Lausanne, Switzerland*
[5] *Solid State Physics Laboratory, ETH, CH-8093 Zürich, Switzerland*

A study of the pressure effect on the magnetic penetration depth λ in polycrystalline MgB_2 was performed by measuring the temperature dependence of the magnetization under an applied pressure of 0.15 and 1.13 GPa. We found that λ^{-2} at low temperature is only slightly affected by pressure [$\frac{\Delta\lambda^{-2}}{\lambda^{-2}} = 1.5(9)\%$], in contrast to cuprate superconductors, where, in the same range of pressure, a very large effect on λ^{-2} was found. Theoretical estimates indicate that most of the pressure effect on λ^{-2} in MgB_2 arises from the electron-phonon interaction.

PACS numbers: 74.70.Ad, 74.62.Fj, 63.20.Kr, 74.25.Ha

Shortly after the discovery of the superconductivity in MgB_2 at 39 K, several investigations of the pressure dependence of the superconducting critical temperature T_c were carried out.[1,2,3,4] Indeed, the magnitude and sign of dT_c/dp may indicate a way to rise T_c at ambient pressure, and moreover, help to understand the superconducting pairing mechanism. So far, all these studies show that T_c decreases with increasing pressure, with a rate depending on the method and the pressure medium used. The first hydrostatic measurement of $T_c(p)$ up to 0.7 GPa, reveals that T_c decreases reversibly under hydrostatic pressure at the rate $dT_c/dp = -1.11(2)$ K/GPa.[4] The behavior of $T_c(p)$ with pressure in MgB_2 was attributed to the pressure induced lattice stiffening (increase of the phonon frequency),[5,6] rather than to the decrease in the electronic density of states $N(E_F)$, that is only moderately affected by pressure.[7] Comparison with theoretical calculations supported the view that MgB_2 is a BCS superconductor with moderately strong electron-phonon coupling.[5]

Apart from T_c, an other relevant superconducting parameter is the magnetic field penetration depth λ. In fact the so-called superfluid density λ^{-2} is related to the Fermi velocity and to the density of charge carriers, and its temperature dependence gives information on the symmetry and on the magnitude of the superconducting gap. A study of pressure effects on $\lambda^{-2}(0)$ can give important informations on how the electronic degrees of freedom are affected by lattice modifications and on the nature of the electron-phonon coupling. Indeed, in cuprates high temperature superconductors (HTS), a huge pressure effect on $\lambda^{-2}(0)$ was found, in particular in $YBa_2Cu_4O_8$ (Y124).[8] Part of this effect was attributed to the strong renormalization of the Fermi velocity, and therefore to the effective mass, due to the non-adiabatic coupling of the electrons to the lattice. This result is in agreement with the substantial oxygen isotope effect found in cuprates[9,10,11,12,13] and can be interpreted in the framework of non-adiabatic theory of superconductivity.[14]

In this paper we report measurements of the magnetic penetration depth under pressure in polycrystalline MgB_2. The temperature dependence of $\lambda^{-2}(T)$ was extracted from the Meissner fraction f measured in a low magnetic field. A small pressure (p) effect on $\lambda^{-2}(0)$ was found [$\frac{\Delta\lambda^{-2}}{\lambda^{-2}} = 1.5(9)\%$], for pressure ranging from 0.15 to 1.13 GPa. Theoretical calculations of the pressure effect on $\lambda(0)$ confirm the smallness of this effect [$\frac{\Delta\lambda^{-2}}{\lambda^{-2}} \simeq 1.4\%$]. These results contrast with the huge effect (~ 40 %) on $\lambda^{-2}(0)$ found in the non-adiabatic cuprate superconductor Y124 in the same range of pressure[8].

The MgB_2 powder sample was prepared by solid state reaction in flowing argon. As starting materials we used Mg flakes and amorphous boron (Alfa Aesar). A pellet with starting composition $Mg_{1.1}B_2$ was placed in a BN crucible and fired in a tube furnace under pure Ar gas. The sample was heated for one hour at 600°C, one hour at 800°C, and one hour at 900°C.

The sample was first ground and then sieved in order to obtain a small grain size R<10 μm, needed for the determination of λ from the Meissner fraction measurements. The hydrostatic pressure was produced in a copper-beryllium piston cylinder clamp, especially designed for magnetization measurements under pressure (see Ref [15]). The sample was put in a teflon cylinder and the pressure cell was then filled with Fluorinert FC77 as pressure transmitting medium. The Meissner fraction was calculated from low field magnetization measurements (field cooling) performed with a commercial Superconducting Quantum Interference Device. In the approximation of spherical grains with average radius R, the Meissner fraction can be related to the magnetic penetration depth via the Shoenberg formula:[16]

$$\frac{\chi}{\chi_0} = \left[1 - 3\left(\frac{\lambda(T)}{R}\right)\coth\left(\frac{R}{\lambda(T)}\right) + 3\left(\frac{\lambda(T)}{R}\right)^2\right]. \quad (1)$$

Any change in χ/χ_0 due to pressure can be attributed mainly to a change of $\lambda(T)$, rather than to a change of R, which is practically pressure independent. The sam-

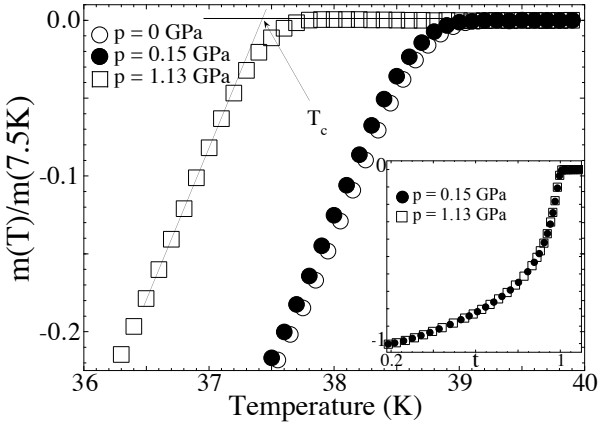

FIG. 1: Field cooled (0.5 mT) normalized magnetization of MgB_2 as a function of temperature in the vicinity of T_c for p_Z (open circles), p_L (filled circles), and p_H (open squares). The inset show the full normalized magnetization data for p_L and p_H as a function of the reduced temperature $t = T/T_c$. Note that some of the data points were dropped for clarity.

ple was measured at low pressure $p_L = 0.15$ GPa and at the highest pressure available $p_H = 1.13$ GPa. The pressure values were determined from a preliminary calibration measurement, where the same sample was measured in the pressure cell together with a small piece of lead. The pressure was detected by measuring the T_c shift of lead (T_c(0kbar)=7.2K). We found $dT_c/dp = -1.24(5)$ K/GPa, in good agreement with previous results.[4] The real zero-pressure measurement could not be performed in the pressure cell, since, in order to seal the cell, at least a small pressure had to be applied.

In Fig. 1 the temperature dependence of the normalized magnetization of MgB_2 at p_L and p_H is shown in the vicinity of T_c, together with the zero pressure p_Z measurement performed on the same sample in a quartz tube. The T_c's were obtained from the intercept of the linear extrapolations (see Fig.1): $T_c(p_Z) = 38.73(3)$ K, $T_c(p_L) = 38.66(3)$ K, $T_c(p_H) = 37.43(3)$ K. The magnetization curves shift systematically with increasing pressure towards lower temperature. In the inset of Fig.1 we show the normalized magnetization as a function of the reduced temperature $t = T/T_c$ for p_L and p_H. The identical temperature dependences for both pressure values indicate the absence of stresses in the sample due to pressure.

From the magnetization the Meissner fraction was extracted. Because of the unknown mass of the sample in the pressure cell, the Meissner fraction for the lowest pressure (p_L=1.5 kbar) was normalized at low temperature with the value obtained by measuring the same sample in a quartz tube at zero pressure p_Z. The values of λ^{-2} were then calculated using the Shoenberg formula (Eq. (1)). The p_Z and p_L data were normalized at low temperature to the absolute value of λ^{-2} measured with the muon spin rotation technique (μSR) on the same sample at zero pressure.[17]

We define the shift of λ^{-2} between two different pressures p_L (lower) and p_H (higher) at a temperature T as:

$$\frac{\Delta\lambda^{-2}}{\lambda^{-2}} \equiv \frac{\lambda^{-2}(p_H,T) - \lambda^{-2}(p_L,T)}{\lambda^{-2}(p_L,T)} \qquad (2)$$

The temperature dependences of λ^{-2} for p_L and p_H, are shown in Fig. 2, together with the p_Z data measured in the quartz tube. The $\lambda^{-2}(T)$ curves for p_Z and p_L overlap perfectly for temperatures not too close to T_c, where a small pressure shift is present. Unfortunately, we were not able to obtain reliable data below 7K because of a large background signal due to lead impurities in the pressure cell. Therefore, while for the p_Z measurement in the quartz tube we show the data down to 2 K, for the p_L and the p_H measurements we show the data only down to 7 K (see lower panel of Fig. 2). Due to the pressure effect on T_c, the curves for p_L and p_H are clearly distinct at high temperature, but they merge at low temperature. The error bars on λ^{-2} (not shown) were determined considering that magnetization measurements are reproducible within ≈ 0.5 %.

The shift of λ^{-2} at the lowest temperature available $T \simeq 7$ K between $p_L = 0.15$ GPa and $p_H = 1.13$ GPa (see Eq. 2) is: $\Delta\lambda^{-2}/\lambda^{-2} = 1.2(1.1)\%$. This result shows that only a very small pressure effect on λ^{-2} is present. The pressure results are summarized in Table I.

To determine the pressure effect on the zero temperature $\lambda^{-2}(0)$, a fit to the experimental data is needed. It was well established that MgB_2 is a two band superconductor with two superconducting gaps of different size, the larger one originating from the 2D σ-band and the smaller one from the 3D π-band[18,19,20,21]. Taking this into account, the temperature dependence of λ, in the low temperature range, can be written in the form[22]:

$$\lambda^{-2}(T) = \lambda^{-2}(0)\left[1 - w\left(\frac{2\pi\Delta_1(0)}{k_BT}\right)^{1/2}\exp\left(-\frac{\Delta_1(0)}{k_BT}\right) - (1-w)\left(\frac{2\pi\Delta_2(0)}{k_BT}\right)^{1/2}\exp\left(-\frac{\Delta_2(0)}{k_BT}\right)\right] \qquad (3)$$

Here, Δ_1 and Δ_2 are the zero temperature small and large gap associated to the π and σ bands, respectively, and $w = \lambda_1^{-2}(0)/\lambda^{-2}(0)$.

The zero pressure data were then fitted to Eq. 3 up to 22 K. The fit gave the following results: $\lambda^{-2}(0) = 91.1(2)$ μ m^{-2}, $w = 0.22(3)$; $\Delta_1 = 2.3(2)$ meV, $\Delta_2 = 7.4(4)$ meV. The estimated gaps are in good agreement with previous results from penetration depth measurements[22,23].

Because of the lack of data below 7 K for p_L and p_H, these data were analysed with fixed w obtained from the fit to the zero-pressure data. Here it is assumed that w is not affected by pressure up to 1.13 GPa. This assumption will be shown below to be correct by our model calculations [see Eq.(8)]. The other fitting parameters ($\lambda^{-2}(0)$ and the gaps) were left free. As shown by the

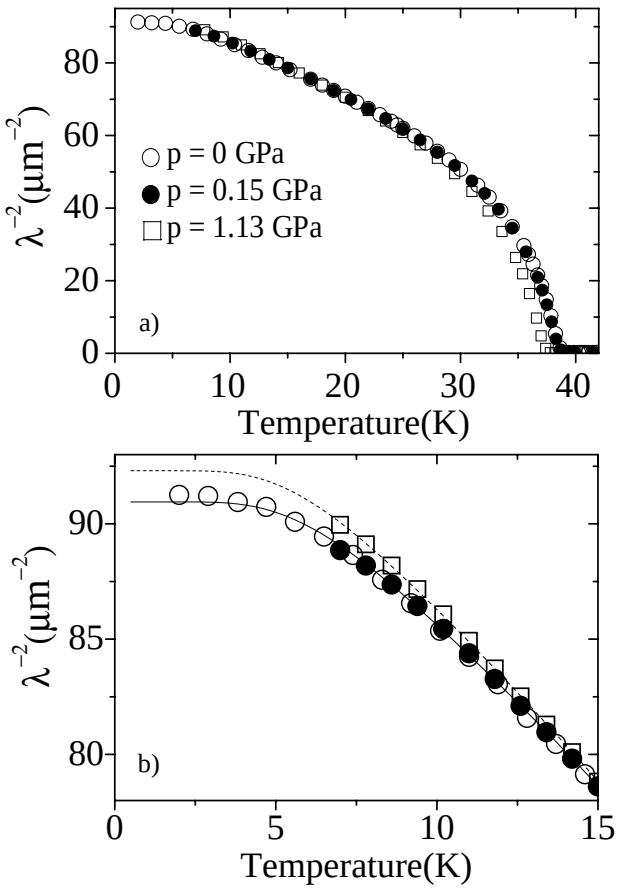

FIG. 2: a) λ^{-2} as a function of temperature for $p_Z = 0$ GPa (open circles), $p_L = 0.15$ GPa (filled circles), and $p_H = 1.13$ GPa (open squares). b) Low temperature region on a larger scale. The error bars (not shown) for temperatures below 10 K, are about two times the symbol size and decrease with increasing temperature. The solid and dashed lines are fits to the p_L and p_H data, respectively, using Eq. 3. Note that the data points are much more dense than what is shown in this figure, since part of them were dropped for clarity.

solid and dashed lines in panel b) of Fig. 2, the data are well described by Eq. (3). In particular the fitted curve of the p_L data (solid line) follows very well the p_Z data below 7 K, as expected. The fit yields for $\lambda^{-2}(0)$: $\lambda^{-2}(0)_{p_L} = 90.9(5)\mu m^{-2}$ and $\lambda^{-2}(0)_{p_H} = 92.3(6)\mu m^{-2}$ (see Table II). So that the relative shift of λ^{-2} at $T = 0$ between $p_L = 1.5$ kbar and $p_H = 11.3$ kbar is [see Eq. (2)]:

$$\frac{\Delta\lambda^{-2}}{\lambda^{-2}} = 1.5(9)\% \qquad (4)$$

This result indicates that there is a small, but not zero, pressure effect on the magnetic penetration depth at 0 K in the range $p = 0.15$ - 1.13 GPa. A summary of the pressure results are reported in Table I. All the fitting parameters are summarized in the Table II. The two gaps show a small decrease with increasing pressure, in agreement with the corresponding decrease of T_c. In Table II we added also the ratio $2\Delta/k_BT_c$ calculated for Δ_1 and Δ_2 at each pressure. This ratio results to be pressure independent within errors.

TABLE I: Summary of the experimental and theoretical estimations of the pressure shift of λ^{-2}.

	T (K)	p_L (GPa)	p_H (GPa)	$\frac{\lambda^{-2}(p_H,T)-\lambda^{-2}(p_L,T)}{\lambda^{-2}(p_L,T)}$ %
exper.	$\simeq$7	0.15	1.13	1.2(1.1)
fit	0	0.15	1.13	1.5(9)
theory	0	0.15	1.13	$\simeq 1.4 \div 1.7$

Considering that $p_H - p_L \simeq 1$ GPa, Eq. (4) indicates that $d\ln\lambda^{-2}(0)/dp$ is of the order of few %/GPa. Since $\lambda^{-2}(0)$ is proportional to the squared plasma frequency, ω_p^2, then a free electron gas estimate would give $d\ln\lambda^{-2}(0)/dp = 1/B \simeq 0.65\%$/GPa, where we have used $\omega_p^2 \propto 1/\Omega$, being $B = -dp/d\ln\Omega \simeq 155$ GPa the bulk modulus of MgB_2,[6] and Ω the volume of the unit cell. As we show below, an improved estimate which takes into account MgB_2 band structure effects does not change much the free electron gas result. Let us consider the zero temperature expression of the penetration depth:[25]

$$\lambda^{-2}(0) = \frac{e^2}{3\hbar\pi^2c^2}\sum_n \oint_{S_F^n} ds|\mathbf{v}_n(s)|, \qquad (5)$$

where the integral runs over the Fermi surface S_F^n of the n-th band ($n = \sigma, \pi$) and $\mathbf{v}_n(s)$ is the corresponding surface bare electron velocity vector. Let us use the model of Ref. 26 where the π bands are modeled by a half-torus Fermi surface of area S_1 and Fermi velocity v_1, while the σ bands are approximated by a cylindrical Fermi surface of area S_2 and Fermi velocity v_2. Equation (5) then reduces simply to $\lambda^{-2}(0) = \lambda_1^{-2}(0) + \lambda_2^{-2}(0)$, where $\lambda_i^{-2}(0) \propto S_iv_i$, $i = 1, 2$, and

$$\frac{d\ln\lambda^{-2}(0)}{dp} = w\frac{d\ln\lambda_1^{-2}(0)}{dp} + (1-w)\frac{d\ln\lambda_2^{-2}(0)}{dp}, \qquad (6)$$

where $w = \lambda_1^{-2}(0)/\lambda^{-2}(0) = S_1v_1/(S_1v_1 + S_2v_2)$ is the parameter introduced in Eq.(3). Within the same approximations, the electron density of states at the Fermi level reads $N_F = N_1 + N_2$, where $N_i \propto \Omega S_i/v_i$ is the partial density of states for the band $i = 1, 2$. Therefore, since $\lambda_i^{-2}(0) \propto S_iv_i \propto \Omega S_i^2/N_i$, and considering that S_1 and S_2 scale as $\Omega^{-2/3}$, Eq.(6) reduces to:

$$\frac{d\ln\lambda^{-2}(0)}{dp} = \frac{1}{3B} - \left[\frac{1-w+\eta w}{\eta+(1-\eta)N_2/N_F}\right]\frac{d\ln N_F}{dp}, \qquad (7)$$

where we have introduced the parameter $\eta = (d\ln N_1/dp)/(d\ln N_2/dp)$ whose calculated value ranges between $\eta \simeq 1$,[27] and $\eta \simeq 0$.[28] Hence, by setting $d\ln N_F/dp \simeq -0.31\%$/GPa,[7] $w = 0.22$, and $N_2/N_F \simeq$

TABLE II: Fitting parameters obtained from the fit of the experimental data showed in Fig. 2 by the Eq. (3).

p GPa	$\lambda^{-2}(0)$ (μm^{-2})	$\Delta_1(0)$ (meV)	$\Delta_2(0)$ (meV)	w	$2\Delta_1(0)/k_BT_c$	$2\Delta_2(0)/k_BT_c$
0	91.1(2)	2.3(2)	7.4(4)	0.22(3)	1.38(12)	4.43(24)
0.15	90.9(5)	2.4(1)	7.3(1)		1.44(6)	4.38(6)
1.13	92.3(6)	2.3(1)	7.0(1)		1.43(6)	4.34(6)

0.4,[29] from Eq.(7) we obtain $d\ln\lambda^{-2}(0)/dp \simeq 0.8\%$/GPa or 0.5%/GPa according to whether $\eta = 0$ or $\eta = 1$, respectively. By the same token, it is easy to show that:

$$\frac{dw}{dp} = \frac{w(1-w)(1-\eta)}{\eta + (1-\eta)N_2/N_F}\frac{d\ln N_F}{dp} \simeq (0 \div -0.1)\%/\text{GPa}, \quad (8)$$

confirming the assumption $dw/dp = 0$ used in obtaining Eq.(4).

Our estimate $\Delta\lambda^{-2}/\lambda^{-2} \simeq (0.5 \div 0.8)\%$ does not deviate from the free eletron gas result, suggesting that other factors than band structure should be considered in order to explain the measured value reported in Eq.(4). It is then natural to consider the electron-phonon interaction λ_{el-ph}. The pressure effect on λ_{el-ph} in MgB_2 is mainly due to a pressure induced hardening of the optical phonon modes. The electron-phonon renormalized penetration depth is $\lambda^{*-2}(0) = \lambda^{-2}(0)/(1+\lambda_{el-ph})$, where $\lambda^{-2}(0)$ is the bare quantity we have considered before. Hence:

$$\frac{d\ln\lambda^{*-2}(0)}{dp} \simeq (0.5 \div 0.8)\%/\text{GPa} - \frac{\lambda_{e-ph}}{1+\lambda_{e-ph}}\frac{d\ln\lambda_{e-ph}}{dp}, \quad (9)$$

which, by using $d\ln\lambda_{e-ph}/dp \simeq -1.7\%$/GPa,[7] and $\lambda_{el-ph} \simeq 1$,[29] corresponds to $\Delta\lambda^{-2}/\lambda^{-2} \simeq (1.4 \div 1.7)\%$, in better agreement with Eq.(4). This simple analysis evidences therefore that the electron-phonon interaction provides the main contribution to the pressure effect on the zero temperature penetration depth. This theoretical estimate of the pressure shift of $\lambda(0)^{-2}$ is reported in the Table I for a direct comparison with the experimental finding.

Similar experiment on the Y124, in the same range of pressure, gives a very large effect on $\lambda(0)^{-2}$ ($\sim 40\%$).[8] Arguments are used there to deduce that part ($\sim 30\%$) of this large effect is due to the pressure dependence of the Fermi velocity, because of the non-adiabatic electron-lattice coupling. From the results of the present work, we can therefore argue that such non-adiabatic effects on $\lambda(0)^{-2}$ are negligible in MgB_2, as previously demonstrated by μSR measurements.[30]

In summary, we studied the pressure effect on the magnetic penetration depth at low temperature in polycrystalline MgB_2. We found that pressure up to 1.13 GPa induces a small positive change in $\lambda(0)^{-2}$ [$\frac{\Delta\lambda^{-2}}{\lambda^{-2}} = 1.5(9)\%$], which is suggested to be due mostly to a pressure change of the electron-phonon coupling.

The authors are grateful to S. Kohout for the help during the measurements, T. Schneider for very fruitful discussions, R. Brutsch and D. Gavillet for the measurements of the grain size distribution of the powder sample. This work was supported by the Swiss National Science Foundation and partly by the NCCR Program MaNEP sponsored by the Swiss National Science Foundation.

* Email: dicastro@physik.unizh.ch

1 M. Monteverde *et al.*, Science **292**, 75 (2001).
2 B. Lorenz, R. L. Meng, and C. W. Chu, Phys. Rev. B **64**, 012507 (2001).
3 E. Saito *et al.*, J. Phys. Condens. Matter **13**, L267 (2001).
4 T. Tomita *et al.*, Phys. Rev. B **64**, 092505 (2001).
5 S. Deemyad *et al.*, Physica C, **385**, 105 (2003).
6 A. F. Goncharov *et al.*, Phys. Rev. B **64**, 100509(R) (2001).
7 I. Loa and K. Syassen, Solid State Commun. **118**, 279 (2001)
8 R. Khasanov, J. Karpinski, and H. Keller, cond-mat/0405643.
9 G. M. Zhao and D. E. Morris, Phys. Rev. B **51**, 16487 (1995).
10 J. Hofer *et al.*, Phys. Rev. Lett. **84**, 4192 (2000).
11 R. Khasanov *et al.*, J. Phys.: Condens. Matter **15**, L17 (2003).
12 R. Khasanov *et al.*, Phys. Rev. Lett. **92**, 057602 (2004).
13 R. Khasanov *et al.*, Phys. Rev. B **68**, 220506(R) (2003).
14 C. Grimaldi, E. Cappelluti, and L. Pietronero, Europhys. Lett. **42**, 667 (1998).
15 T. Strässle, Ph.D. Thesis, ETH Zürich (2001).
16 D. Shoenberg, Proc. R. Soc. Lond. A **175** , 49 (1940).
17 D. Di Castro *et al.*, unpublished.
18 R. S. Gonnelli *et al.*, Phys. Rev. Lett. **89**, 247004 (2002).
19 F. Bouquet *et al.*, Phys. Rev. Lett. **87**, 047001 (2001).
20 P. Szabo *et al.*, Phys. Rev. Lett. **87**, 137005 (2001).
21 S. Souma *et al.*, Nature **423**, 65 (2003).
22 M-S. Kim *et al.*, Phys. Rev. B **66**, 064511 (2002).
23 F. Manzano *et al.*, Phys. Rev. Lett. **88**, 047002 (2002).
24 H. J. Choi *et al.*, Nature **418**, 758 (2002).
25 A. Carrington and F. Manzano, Physica C **385**, 205 (2003).
26 T. Dahm and N. Schopohl, Phys. Rev. Lett. **91**, 017001 (2003).

[27] N. I. Medvedeva *et al.*, Phys. Rev. B **65**, 052501 (2001).
[28] T. Vogt *et al.*, Phys. Rev. B **63**, 220505(R) (2001).
[29] A. Y. Liu, I. I. Mazin, and J. Kortus, Phys. Rev. Lett. **87**, 087005 (2001).
[30] D. Di Castro *et al.*, Phys. Rev. B **70**, 014519 (2004).